Development and characterization of biological sutures made of cell-assembled extracellular matrix

Paul Borchiellini, Adeline Rames, François Roubertie, Nicolas L'heureux, Fabien Kawecki

IOP Publishing Biofabrication 15 (2023) 045018 https://doi.org/10.1088/1758-5090/acf1cf

Biofabrication

OPEN ACCESS

RECEIVED
23 June 2023

REVISED
11 August 2023

ACCEPTED FOR PUBLICATION
18 August 2023

PUBLISHED
31 August 2023

PAPER

Development and characterization of biological sutures made of cell-assembled extracellular matrix

Paul Borchiellini[1], **Adeline Rames**[1], **François Roubertie**[2,3], **Nicolas L'Heureux**[1] and **Fabien Kawecki**[1,*]

[1] Univ. Bordeaux, INSERM, BIOTIS, UMR1026, Bordeaux F-33000, France
[2] IHU Liryc, Electrophysiology and Heart Modeling Institute, Pessac, France
[3] Congenital Heart Diseases Department, CHU de Bordeaux, Pessac, France
[*] Author to whom any correspondence should be addressed.

E-mail: fabien.kawecki@inserm.fr

Keywords: biological suture, cell-assembled extracellular matrix, anastomosis, human textiles

Supplementary material for this article is available online

Abstract

Most vascular surgical repair procedures, such as vessel anastomoses, requires using suture materials that are mechanically efficient and accepted by the patient's body. These materials are essentially composed of synthetic polymers, such as polypropylene (Prolene^{TM}) or polyglactin (Vicryl^{TM}). However, once implanted in patients, they are recognized as foreign bodies, and the patient's immune system will degrade, encapsulate, or even expel them. In this study, we developed innovative biological sutures for cardiovascular surgical repairs using Cell-Assembled extracellular Matrix (CAM)-based ribbons. After a mechanical characterization of the CAM-based ribbons, sutures were made with hydrated or twisted/dried ribbons with an initial width of 2 or 3 mm. These biological sutures were mechanically characterized and used to anastomose *ex vivo* animal aortas. Data showed that our biological sutures display lower permeability and higher burst resistance than standard Prolene^{TM} suture material. *In vivo* carotid anastomoses realized in sheep demonstrated that our biological sutures are compatible with standard vascular surgery techniques. Echography confirmed the absence of thrombus and perfect homeostasis with no blood leakage was obtained within the first 10 min after closing the anastomosis. Finally, our findings confirmed the effectiveness and clinical relevance of these innovative biological sutures.

1. Introduction

Sutures are the gold standard for most surgical closing and repairs, such as approximating tissues or attaching prostheses [1]. The successful outcome of the suture relies on the behavior of its material within a biological environment. This depends on the intrinsic mechanical properties of the material and its chemical composition. The ideal suture material should provide favorable handling characteristics (strength and flexibility) and superior biological properties (biocompatibility and resorption capacity) [2, 3]. It should be accepted by the patient without rejection or chronic inflammation, resist infection, and be integrated and remodeled by the patient's body.

Synthetic polymers, such as polypropylene (Prolene^{TM}) or polyglactin (Vicryl^{TM}), have been used for decades and remain the gold standard for vascular surgery [4, 5]. However, these synthetic materials are recognized as foreign bodies and generate inflammatory reactions [6–8]. While intense efforts have been realized to maximize the biocompatibility of suture materials by modifying the material composition and/or its surface, these new suture materials (polyvinylidene fluoride, ultrafine polyethylene terephthalate (PET), or thermoplastic polyurethane) are still recognized as foreign bodies and can generate intrafilamentous granulomas [9, 10]. Degradable sutures such as Maxon^{TM}, composed of polyglycolic acid and trimethylene carbonate, have been reported for pediatric cardiovascular repairs [11]. Indeed, Reimer *et al* used this suture material to anastomosed tissue-engineered tubular valves with the pulmonary artery of growing lambs [12]. However, they observed calcification at the suture material after 12 weeks of implantation [12]. A clinical case reported that Nylon^{TM} suture material had caused a foreign body reaction resulting in

uncontrolled migration of the material out from its original position [13]. This migration can be associated with complications, such as ulceration, as observed in blepharoptosis surgery [14]. In 2021, Lee *et al* retrospectively compiled the complication rates that occurred after using nonabsorbable PET (or polyester) and Prolene^{TM} suture in a cohort of 229 patients who underwent vaginal uterosacral ligament suspension surgeries [15]. Their results demonstrated that 20.1% (30/149) of the patients treated with Prolene^{TM} sutures and 46.3% (37/80) of the patients treated with PET sutures presented complications (granulation tissue and suture erosion). Furthermore, synthetic suture materials have been shown to be favorable to bacterial biofilm formation [16, 17] and are consequently a source of infection [18]. While the adverse effects of synthetic sutures are poorly described in the literature by few clinical analyses realized on small cohorts, they are commonplace and frequently observed by surgeons in diverse surgical specializations. The severity of these adverse effects is relative to the intensity of the inflammatory reaction or the infection, which can vary between patients, and the location of the suture in the patient's body.

Human and ovine biological materials synthesized in the laboratory by normal dermal fibroblasts in culture has been developed [19–24]. This material, called Cell-Assembled extracellular Matrix (CAM), is produced in large culture flasks as a sheet, which can be cut into ribbons that can be assembled in biological textiles [21, 22, 25]. This biomaterial was successfully implanted in humans as tubes for vascular applications [26–28]. Implantation results validated the hypothesis that this completely biological material can integrate with native tissue, be remodeled by the host's cells, and resist infection. Data have also shown that CAM produced by allogeneic fibroblasts (from a donor) does not elicit an immune response [27]. Recent data demonstrated that CAM material can be devitalized (frozen/thawed and dehydrated/rehydrated) without damaging its structure [21], is compatible with standard sterilization processes (ethylene oxide or supercritical CO_2 gas expositions), and remains stable for at least one year using frozen/dry storage [29]. In addition, it has been demonstrated that human CAM-based ribbons are long-lived *in vivo* (up to six months) and do not trigger a degradative immune response but show a very slow remodeling [30]. These data open the door to a non-living and allogeneic production strategy of CAM-based material that is available on-demand and more economically feasible compared to autologous products containing living cells.

In this study, we developed an innovative biological suture made of an allogeneic devitalized CAM material and, as an example of application, we tested its usability for vascular anastomosis. We first demonstrated that we can adapt the CAM sheet properties (strength, hydroxyproline content, and thickness) by controlling the time of culture to produce strong sutures. Thereafter, we considered two double-spiral cutting patterns for making 2 and 3 mm-wide ribbons. We first evaluated the max force of the ribbons along the patterns to define the ideal areas for suture production and we characterized the mechanical properties of the ribbons. Then, we designed two models of biological suture by crimping eyeless surgical needles with 16 week-old hydrated or twisted/dried CAM-based ribbons with an initial width of 2 or 3 mm. We mechanically characterized these models by realizing *ex vivo* anastomoses of animal aortas. Finally, *in vivo* carotid anastomoses were performed in sheep to demonstrate that our biological suture is compatible with standard vascular surgery techniques in a clinically relevant setting.

2. Materials and methods

2.1. CAM sheet production

Ovine and human skin fibroblast cells were isolated from healthy animals and healthy adult patients (in accordance with article L. 1243-3 of the code of public health and under the Agreement DC-2008-412 with the University Hospital Center of Bordeaux, France [update 10 October 2014]) according to our previously described protocols [23, 31]. The fibroblast cells were grown in Dulbecco's modified Eagle medium containing F-12 nutrient mixture (3331-028; Gibco®, Thermo Fisher Scientific, Bordeaux, France) supplemented with fetal bovine serum (FBS) in humidified incubators at 37 °C with 5% CO_2 and frozen after four amplification steps. Ovine and human fibroblasts were cultured using medium containing 20% FBS (HyClone SH30109.03, GE Healthcare Life Science, Issaquah, WA, USA) and a combination of FBS (10% Hyclone + 10% Biowest S1810.500, Nuaillé, France), respectively. For the CAM sheet production, frozen cells were thawed in passage 4 (P4) and amplified twice in 175 cm^2 flasks for 1 week until P6. Then, fibroblast cells were seeded at a density of 1×10^4 cells cm^{-2} (P7) in 225 cm^2 flasks and cultured for 8 and 16 weeks in a medium supplemented with 500 μM of sodium L-ascorbate (A4034-500G; Sigma-Aldrich, Saint-Quentin-Fallavier, France). CAM sheets were also produced within 6-well-plates in the same condition for perforation assay, hydroxyproline quantity quantification, thickness measurement, and histological staining. The media was changed three times per week. At the end of the culture times (8 and 16 weeks), CAM sheets were quickly rinsed in sterile distilled water and frozen at −80 °C until their use.

2.2. Perforation assay

The strength of the ovine and human CAM sheets cultured for 8 and 16 weeks was evaluated using a perforation test in accordance with the ISO

7198:1998/2001 standard, as previously described [23]. The CAM sheets cultured within 6-well-plates were manually detached from the plastic and positioned on a custom-made clamping device. The strength was measured by perforating tissues until rupture with a 9.8 mm-diameter spherical Teflon® indenter at a constant displacement rate of 20 mm min^{-1} (n = 12–24 tissues by time of culture by species).

2.3. Hydroxyproline quantification

Hydroxyproline content in ovine and human CAM sheets cultured for 8 and 16 weeks was quantified using a hydroxyproline assay as previously described [24]. Briefly, 8 mm-diameter punch samples (6.2 mm^2) of CAM were dried at room temperature overnight. The samples were rehydrated for 30 min using 100 μl of distilled water. Subsequently, the samples were hydrolyzed with 100 μl of 10 N sodium hydroxide (NaOH; Sigma-Aldrich) at 120 °C for 1 h. The hydrolysis was stopped by neutralizing the lysate with 100 μl of 10 N hydrochloride acid (HCl; Honeywell—Fluka, Seelze, Germany). The lysates and the trans-4-hydroxy-L-proline standards (Santa Cruz, Heidelberg, Germany; calibration range: 0.25, 0.5, 1, 2, 4, and 8 μg) were loaded in a 96-well-plate in duplicate and dried at 65 °C for 2 h. The evaporated samples and standards were incubated with 100 μl of 0.05 M chloramine-T (Sigma-Aldrich) for 20 min. Then, the samples and standards were incubated with 100 μl of 1 M Ehrlich's solution at 65 °C for 20 min. Finally, the photocolorimetric reaction was stopped by placing the plate on ice for 5 min, and the absorbance was measured at 550 nm using a VICTOR multilabel plate reader (PerkinElmer, Villebon-sur-Yvette, France) (n = 8–17 tissues by time of culture by species).

2.4. CAM thickness measurement

The thickness of hydrated ovine and human CAM samples cultured for 8 and 16 weeks was measured with a laser micrometer (Xactum, Aeroel, Pradamano, Italia). Samples were placed around a mandrel and positioned between the detectors. Measurement of the mandrel diameter permits the determination of the thickness of each sample using this equation: *sample thickness = (sample around mandrel diameter—mandrel diameter)/2* (n = 72–155 tissues by time of culture by species).

2.5. Histology

Samples of 8 and 16 week-old ovine CAM sheets and anastomosed aortas were fixed overnight in 4% paraformaldehyde, rinsed, dehydrated, and paraffin-embedded. Seven μm-thick paraffin-embedded sample sections were colored with Masson's trichrome staining. Images were captured using an Eclipse 80i microscope (Nikon, Tokyo, Japan).

2.6. CAM-based ribbon production

For ribbon production, frozen 8 and 16 week-old ovine and human CAM sheets were thawed and quickly rinsed in sterile distilled water. Subsequently, the sheets were positioned onto plastic sheets with 2 and 3 mm-wide double-spiral cutting patterns and air-dried under the sterile flow of a biosafety cabinet at room temperature for at least 2 h. The CAM sheets were manually cut using curved scissors following the double-spiral patterns to obtain two long ribbons by pattern. Then, CAM-based ribbons were rehydrated in sterile distilled water and manually detached from the plastic sheet.

2.7. Mapping of the force ribbons over the CAM sheets and mechanical property characterization of the ribbons

For the mapping of the CAM-based ribbon forces, the double-spiral patterns were divided into four sections (a, b, c, and d), and each arc ribbon was numbered (1–19), except the interspiral ribbon. Then, ribbons were mechanically tested to measure their maximal force regarding their location within the sheet. The ribbons were clamped in the jaws of a tensile testing machine (Shimadzu Autograph AGS-X series, Noisiel, France) equipped with a 100 N force sensor, pre-stretched at 20 mm min^{-1} until reaching 0.05 N, and pulled until rupture at the same speed. Data were normalized by the cross-sectional area of each specimen that was measured with a biaxial laser micrometer and processed using a MATLAB code as previously described [29]. The slopes in the quasi-linear region of the stress–strain curves were computed to determine the max force, the ultimate tensile strength (UTS), which represents the maximum stress that can be applied as simple tension to a material before it fails, the strain at break, and the Young's modulus, also called the elastic modulus defined by the ratio of the stress to the elastic deformation caused by the strain (n = 3 CAM sheets by patterns by time points by species).

2.8. CAM-based suture material production

For thread production, hydrated ribbons obtained from 16 week-old ovine CAM sheets cut with the double-spiral patterns (2 or 3 mm-wide) were twisted at five revolutions per centimeter of length as previously described [30]. Then, twisted ribbons were dried under tension for five minutes to reduce the diameter to its minimal size. Diameters of hydrated and twisted/dried CAM-based ribbons (2 and 3 mm-wide) were measured with a laser micrometer (Xactum, Aeroel) (n = 5–8 ribbons by pattern by condition). Four models of biological suture were produced and tested in this study: the ribbons, which are 2 or 3 mm-wide hydrated CAM-based ribbons twisted and dried over the last 5 cm of their extremities, and the twisted ribbons, which are 2 or 3 mm-wide hydrated CAM-based ribbons twisted and dried over their entire length. For the suture production,

each extremity has been crimped with an eyeless surgical needle (ENOVA®, Suturex & Renodex, Carsac-Aillac, France) using a pneumatic attaching machine (QuickyTach III®, Suturex & Renodex). Briefly, the twisted and dried CAM-based ribbon was inserted within the needle hole. Then, the needle was crushed twice (at 0° and 90°) by two half-moon dies.

2.9. Scanning electron microscopy

Samples of biological threads and anastomosed aortas were dried, gold-coated, and observed at an accelerating voltage of 15 kV using a tabletop scanning electron microscope (TM4000Plus, Hitachi, Tokyo, Japan).

2.10. Thread/needle attachment strength measurement

The sutures were mechanically tested to measure the maximal strength of needle attachment in dry condition or after 45 min of rehydration. Briefly, the needle and the thread were clamped to the superior and the inferior jaws of a tensile testing machine (Shimadzu Autograph AGS-X series) equipped with a 100 N force sensor, respectively, in such a way that the crimped part of the needle is completely free of the clamp and in line with the thread pull direction. Then, the sutures were pulled at 20 mm min^{-1} until thread rupture or thread/needle detachment. Values were considered only when the thread slipped out of the needle hole or if the break was at the junction of the thread and the needle ($n = 10$–15 sutures by pattern by condition).

2.11. Breaking load assay

A breaking load assay was realized to measure the resistance to a knot of the four suture models. Briefly, a simple knot was made in the length of hydrated ribbons or twisted/dried ribbons (initial width of 2 or 3 mm). Each end of the threads was clamped between the jaws of a tensile testing machine (Shimadzu Autograph AGS-X series) equipped with a 100 N force sensor and pulled at 20 mm min^{-1} until knot rupture. Values were considered only when the break was at the knot ($n = 5$–9 knots by suture model).

2.12. *Ex vivo* anastomosis

Ex vivo anastomoses were realized using ovine thoracic aortas obtained from sacrificed animals included in another protocol and in accordance with the principles of the 3Rs (replacement, reduction, and refinement) for animal research. Briefly, the 10 cm-long explanted aortas were maintained between two clamps. Collateral vessels were identified and ligatured using 6-0 Prolene™ sutures (Ethicon, Issy-les-Moulineaux, France), and aortas were sectioned in the middle of the interclamp length. Ovine CAM-based sutures (2 and 3 mm-wide hydrated ribbons and twisted/dried ribbons from ovine origin) and 4-0 Prolene™ suture (Ethicon) were used to realize a termino-terminal anastomosis by a parachute approach.

2.13. Permeability assay

Termino-terminal *ex vivo* anastomoses were tested for water permeability. Anastomosed aortas were connected to a home-made perfusion system and exposed to a 200 mmHg internal pressure for 30 s. Water leaked through the anastomosis and the tissue holes generated by the needle passages was collected within a reservoir. The collected volumes were measured, reported to 1 min, and normalized by the number of running stitches ($n = 3$ anastomoses by suture).

2.14. Burst pressure

Termino-terminal *ex vivo* anastomoses were tested for burst pressure. Anastomosed aortas were loaded with a balloon and connected to a homemade bursting bench. Azote gas was injected within the system to inflate the balloon, and pressure was recorded until anastomosis rupture ($n = 3$ anastomoses by suture).

2.15. *In vivo* anastomosis

All protocols and procedures complied with the Principles of Laboratory Animal Care formulated by the National Society for Medical Research which are in-line with the EU Directive 2010/63/EU. In addition, this pre-clinical study was carried out in accredited animal facilities (IHU Liryc, accreditation #A333183), and was approved by the Animal Research Committee (protocol authorization: APAFIS#31724-2021051 911077858). One-year-old sheep were anesthetized using an intravenous propofol bolus injection (1 mg kg^{-1}) and maintained with 1.5%–3% isoflurane during surgery. Skin neck was incised, and carotids were liberated from the surrounding tissues. A bolus of heparin was injected intravenously 5 min before clamping the carotids. Subsequently, the carotids were clamped, sectioned, and anastomosed with a parachute approach. Termino-terminal carotid anastomoses were realized using a biological suture made of a 2 mm-wide hydrated ovine CAM-based ribbon (colored in blue for a better visual on images) or a 6-0 Prolene™ suture (Ethicon) ($n = 4$ animals by suture models). Finally, the clamps were removed, and the blood flow was restored. After 10 min of observation, the surrounding tissue and the cutaneous incision were closed for ultrasound imaging.

2.16. Ultrasound imaging

Echography was realized immediately after the incision closures, approximately 10 min after the anastomoses, using a cardiovascular ultrasound machine (Vivid™ E95, GE Healthcare, Mérignac, France) equipped with a 9L linear transducer (GE Healthcare).

2.17. Statistical analyses

All statistical analyses were performed with GraphPad Prism, Version 9 (GraphPad Software Inc. USA). Data are presented as mean ± standard deviation. Before determining differences between the groups, a Shapiro–Wilk test was realized to evaluate the normal distribution of the data sets. Non-parametric Mann–Whitney tests (for comparing two data sets), parametric unpaired *t*-tests (for comparing two data sets), or one-way analysis of variance with Bonferroni's multiple comparison tests (for comparing four to eight data sets) were used to identify differences. Differences were considered significant at $P < 0.05$.

3. Results

3.1. Impact of the time of culture on the CAM sheet properties

Our approach is based on using a truly biological material called CAM, which is produced as a strong sheet using ovine or human fibroblast cells. The properties of this CAM material (tissue mechanical strength, quantity of hydroxyproline within the tissue, or tissue thickness) can be tightly controlled by varying culture time. This study compared ovine and human CAM sheets cultured for 8 and 16 weeks. By doubling the time of culture, the CAM strength was significantly increased 2.2-fold for ovine CAMs (**** $P < 0.0001$) and 2.1-fold for human CAMs (**** $P < 0.0001$) (figures 1(A) and (B)). Interestingly, ovine and human CAM sheets showed similar perforation strength at 8 and 16 weeks. In addition, culture time doubling resulted in significant augmentations of hydroxyproline quantity (figures 1(C) and (D); ovine CAMs: 2.3-fold, ** $P < 0.01$; human CAMs: 3.1-fold, *** $P < 0.001$) and tissue thickness (figures 1(E) and (F); ovine CAMs: 1.2-fold, **** $P < 0.0001$; human CAMs: two-fold, **** $P < 0.0001$). Interestingly, ovine CAM sheets were thicker than human CAMs sheets when cultured for the same time. A denser and thicker collagenous structure was observed by histological analysis after 16 weeks of culture compared to 8 weeks (figure 1(G)), consistent with the previous measurements.

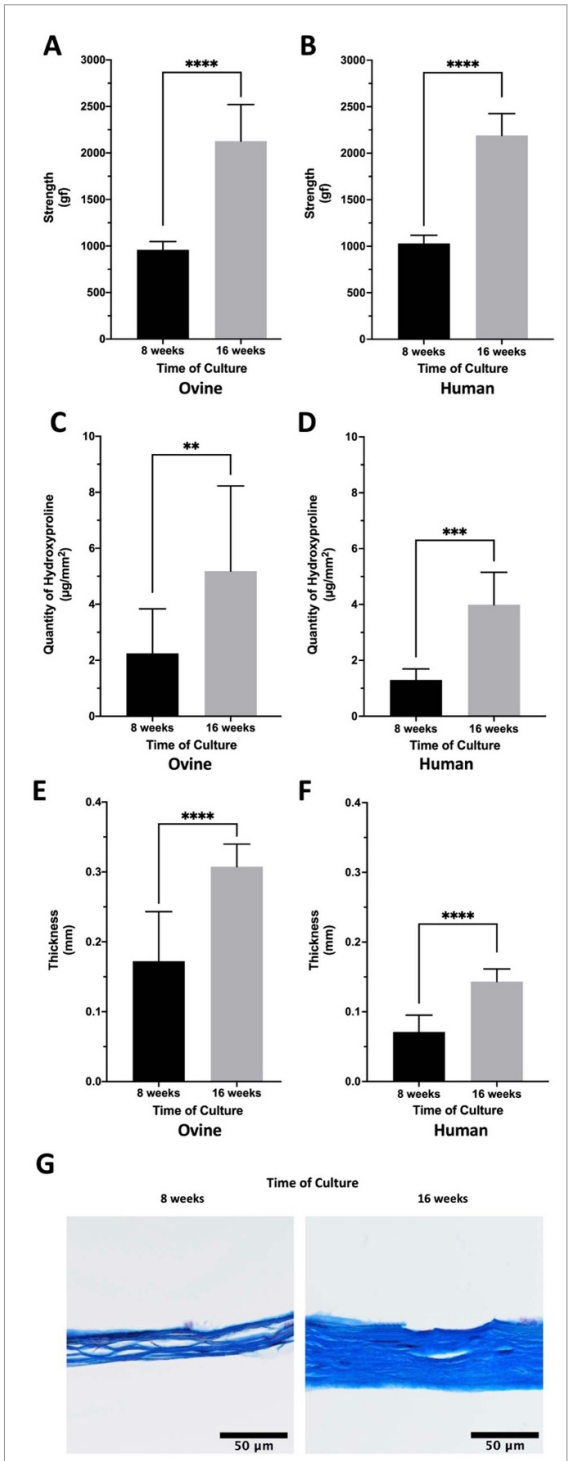

Figure 1. Impact of the culture time on CAM sheet properties. (A)–(F) By doubling the time of culture (8 *vs.* 16 weeks), the strength, the quantity of hydroxyproline, and the thickness of the ovine and human CAM sheets were all significantly increased (significant differences: ** $P < 0.01$; **** $P < 0.0001$). (G) Masson's trichrome staining of cross-sectioned ovine CAM sheets showed a more cohesive and thicker collagenous structure (blue) after 16 weeks of culture compared to 8 weeks. Scale bars; 50 μm.

3.2. Production and characterization of the CAM-based ribbons

We routinely produce CAM sheets with a surface of 19 cm by 10 cm (figure 2(A)). To produce CAM-based ribbons, ovine and human CAM sheets cultured for 8 or 16 weeks were frozen at −80 °C, thawed, and dried onto a plastic sheet containing a double-spiral cutting pattern (figures 2(B) and (C)). After drying, the CAM sheets were stuck to the plastic sheets and cut along the pattern. We choose a double spiral pattern to produce the longest ribbons with the smoothest curves possible to avoid stress concentration points. Our goal was to develop sutures mainly for vascular applications, such as vessel anastomosis. Since this application requires small-diameter sutures, we cut patterns for producing 2 and 3 mm-wide ribbons on ovine and human CAM sheets cultured for

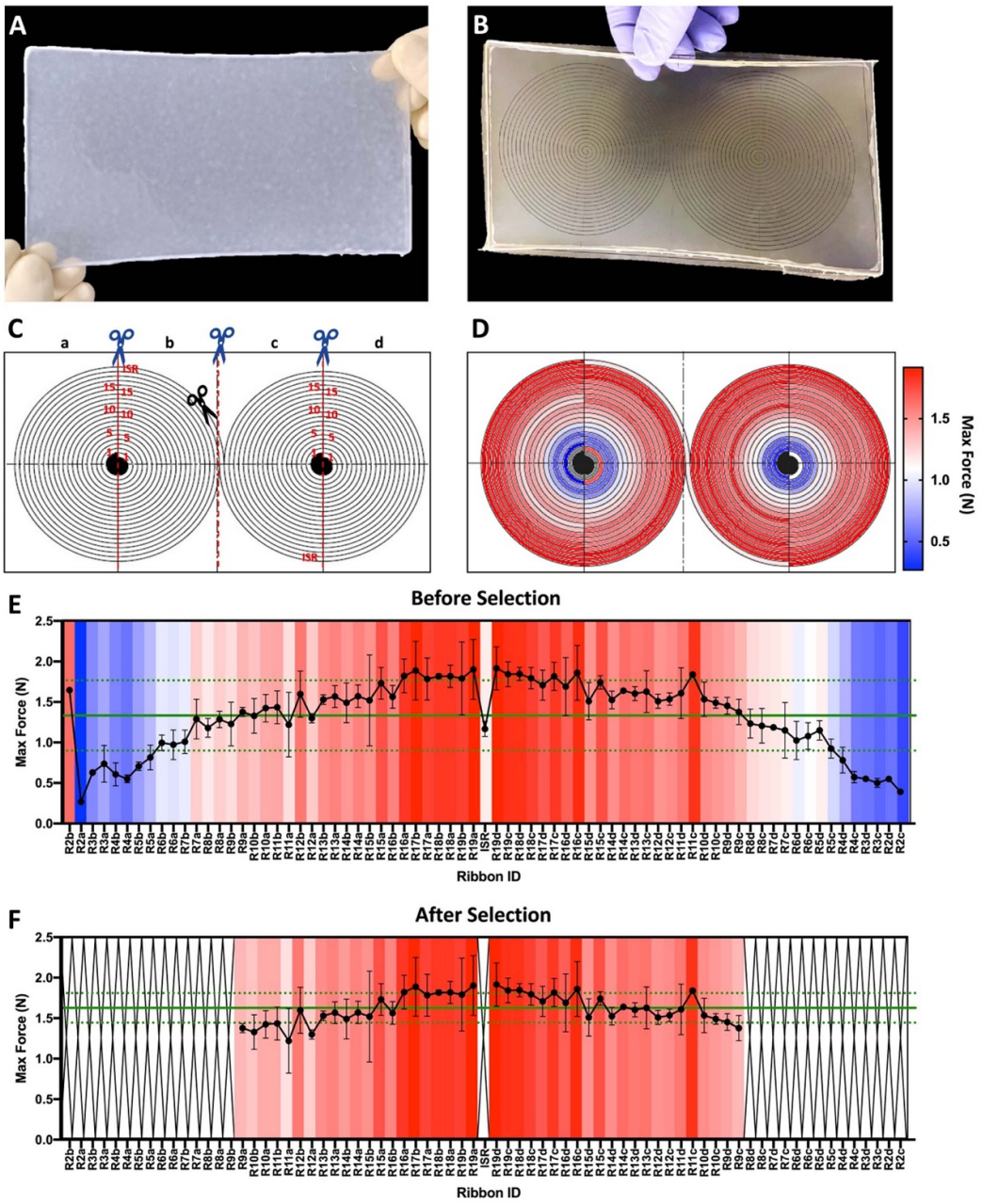

Figure 2. CAM-based ribbon production and maximum force mapping. (A) A fresh 16 week-old CAM sheet of 190 cm^2. (B) The CAM sheet was dried onto a plastic sheet with a double-spiral cutting pattern (2 mm-wide ribbon). (C) Two spirals were cut following the black line (black scissors). For the force mapping, the dried spiral was cut into 180° arcs from four pattern regions (a, b, c, and d), following the red dotted lines (red scissors). Each ribbon arc was numbered (1–19), except the interspiral ribbon (ISR). The black areas were discarded. (D) Heat map of the human CAM-based ribbon max force distribution in the 2 mm-wide double-spiral pattern using a color scale (min. = 0.27 N to max. = 1.9 N). (E) and (F) Max force distribution along the double-spiral ribbon before and after selecting the central part of the human CAM-based ribbon. This selection allowed obtaining two ribbons with increased average force and homogeneity (mean max force: green lines and ± standard deviations: dotted green lines). Black crosses indicate the ribbon sections eliminated for the suture fabrication.

8 and 16 weeks. Then, we tested the uniaxial breaking force of each 180° arc. Mapping of the breaking force confirmed that ribbons located at the center of the spirals, which had the highest curvature, displayed lower breaking forces (figures 2(D), (E) and S1). Since a suture is only as strong as its weakest point, we decided to eliminate sections that are below the mean max force value of the initial ribbon. The selected ribbons displayed a higher and more homogenous average max force and a reduction of the coefficient of variation compared to their initial ribbons (table 1). Mechanical evaluation of the selected CAM-based ribbons demonstrated that by doubling the time of culture (8 *vs.* 16 weeks), the max force of the ovine and human 2 and 3 mm-wide CAM-based ribbons were all significantly increased (2.1- to 2.7-fold, **** $P < 0.0001$) (figure 3(A)). In addition, no significant max force difference was noted between either ovine and human ribbons and 2 and 3 mm-wide ribbons (figure 3(A)).

Table 1. CAM-based ribbons characteristics before and after selection.

			Before selection			After selection				
Origin	Time of culture	Ribbon width	Mean max force ± SD (N)	CV (%)	Spiral length (cm)	Mean max force ± SD (N)	CV (%)	Spiral length (cm)	Mean max force increase (%)	CV reduction (%)
Ovine	8 weeks	2 mm	0.57 ± 0.14	24.8	478	0.60 ± 0.10	16.9	429	5.3	31.8
		3 mm	0.81 ± 0.19	23.9	358	0.88 ± 0.16	18.6	282	8.6	22.2
	16 weeks	2 mm	1.37 ± 0.33	24.0	478	1.43 ± 0.29	20.0	417	4.4	16.7
		3 mm	1.69 ± 0.51	30.3	358	1.81 ± 0.47	25.8	300	7.1	14.9
Human	8 weeks	2 mm	0.55 ± 0.14	24.7	478	0.60 ± 0.13	22.2	367	9.1	10.1
		3 mm	0.66 ± 0.21	31.7	358	0.79 ± 0.16	20.0	142	19.7	36.9
	16 weeks	2 mm	1.39 ± 0.42	30.1	478	1.63 ± 0.26	15.8	361	17.3	47.5
		3 mm	1.55 ± 0.53	34.1	358	1.90 ± 0.31	16.2	222	22.6	52.5

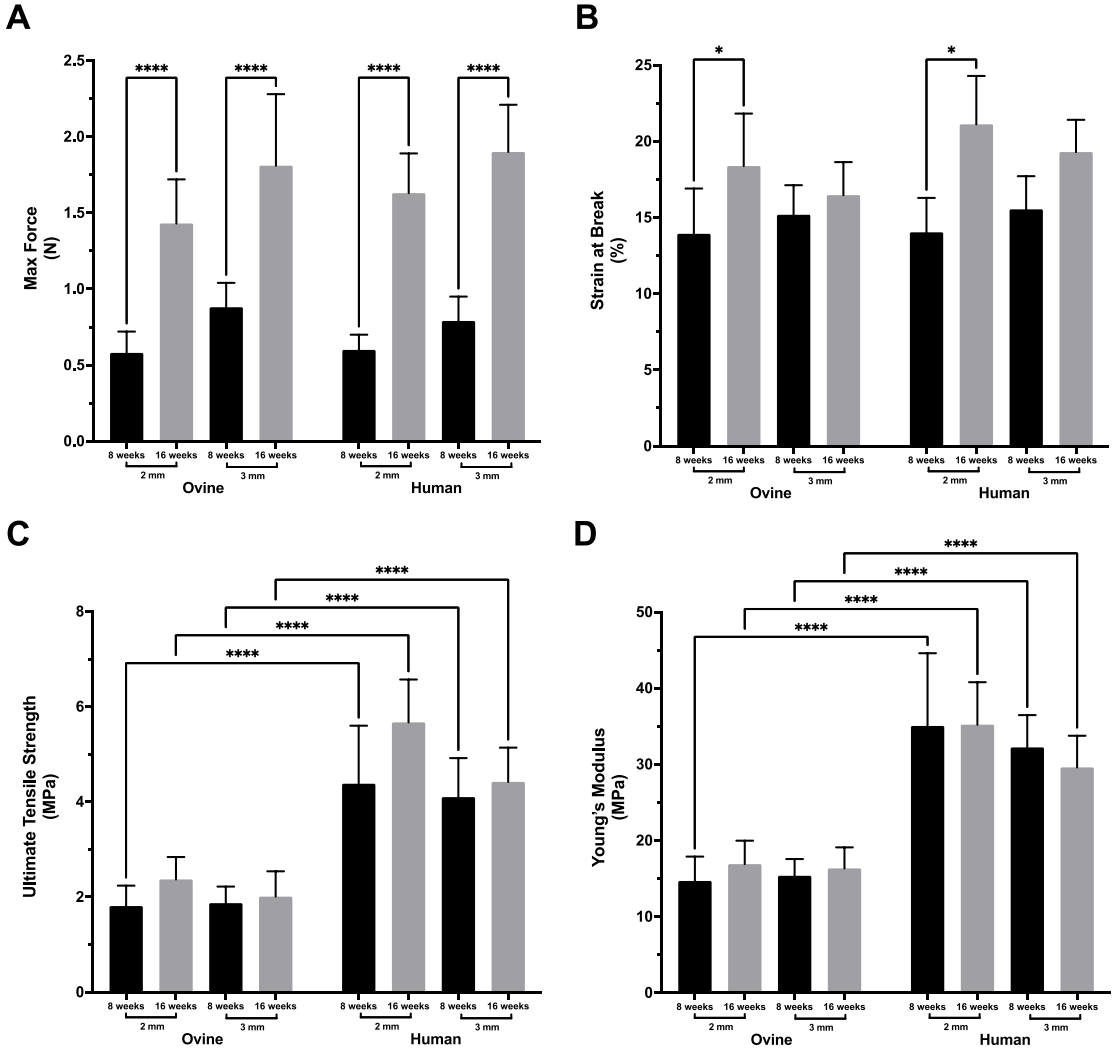

Figure 3. Mechanical evaluation of the selected CAM-based ribbons. Tensile test has been realized to determine the (A) max force, (B) strain at break, (C) ultimate tensile strength, and (D) Young's modulus of 2 and 3 mm-wide hydrated ribbons made of 8 and 16 week-old CAM sheets from ovine and human origins (significant differences: * $P < 0.05$; **** $P < 0.0001$).

After ribbons selection, tensile test data were processed to determine strain at break, the UTS, and Young's modulus of the selected CAM-based ribbons. Low but significant augmentations of the strain at break were measured after doubling the culture time of ovine and human 2 mm-wide ribbons (figure 3(B); ovine 2 mm-wide ribbons: 1.3-fold, * $P < 0.05$; human 2 mm-wide ribbons: 1.5-fold, * $P < 0.05$). As observed for the max force, the species origin and width of the CAM-based ribbons are not playing a role in the strain at break (figure 3(B)). However, data revealed that CAM-based ribbons with human origin displayed significantly higher UTS and Young's modulus compared to those with ovine origin (**** $P < 0.0001$) (figures 3(C) and (D)). As expected, UTS and Young's modulus were not affected by the ribbon width (figures 3(C) and (D)).

3.3. CAM-based ribbon twisting/drying for suture production

Since our goal was to develop an allogeneic biological suture and evaluate its preclinical usability for vessel anastomosis in sheep, further development was focused on using ovine CAM sheets cultured for 16 weeks and cut in 2 and 3 mm-wide ribbons. To insert CAM-based ribbons in eyeless surgical needles, we twisted and dried the ends of the ribbons to create a tread with a minimal diameter (figures 4(A)–(F)). After twisting hydrated ribbons at five revolutions per centimeter of length, the ribbons were dried under tension. A gentle massage of the twisted ribbon during drying allowed a regular distribution of the twists along the thread (figures 4(B) and (E)). While the drying process did not significantly reduce the diameter of the threads (figure 4(G)), it prevented untwisting and made the threads rigid enough to permit good handling for needle crimping. The diameter ranges of 2 and 3 mm-wide twisted/dried ribbons obtained from CAM sheet cultured for 16 weeks were 0.204–0.237 mm and 0.294–0.318 mm, respectively. These diameters correspond to 2 and 3 gauges of the European Pharmacopeia (Ph. Eur.) metric or 4-0 and 3-0 for the United States Pharmacopeia (USP) size of natural suture materials. Scanning electron

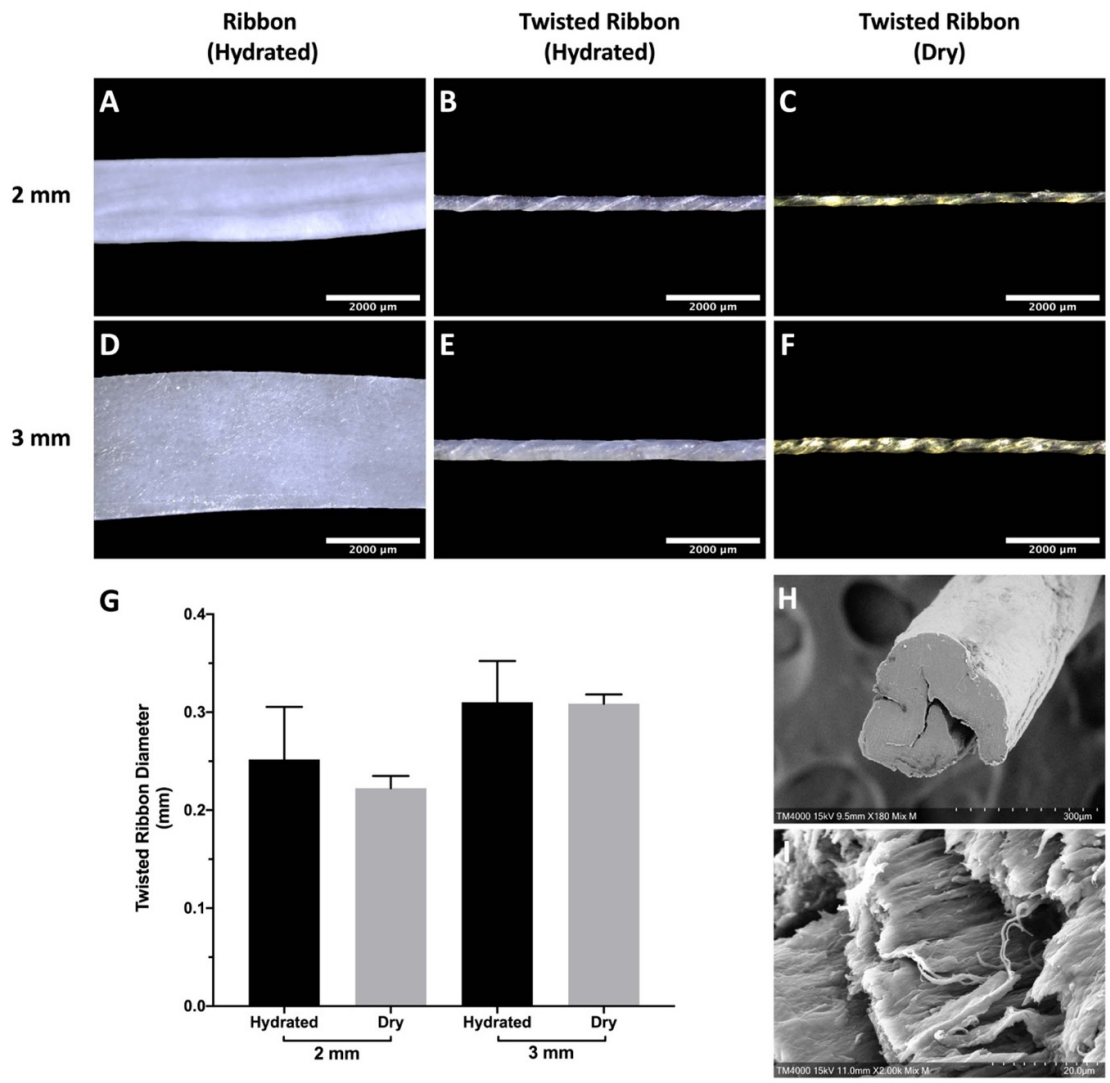

Figure 4. CAM-based ribbon twisting and drying. (A)–(F) To minimize the thread diameter, the 2 and 3 mm-wide hydrated ribbons were twisted at five revolutions per centimeter of length and dried under tension for 5 min under a laminal flood hood. Scale bars; 2000 μm. (G) Twisted ribbon diameter measurements showed non-significant reduction after drying (2 mm-wide ribbons: $P = 0.71$ and 3 mm-wide ribbons: $P > 0.99$). (H) Scanning electron microscopy showing the central part of a 3 mm-wide twisted/dried ribbon that was perpendicularly cut with a scalpel. Scale bar; 300 μm. (I) Scanning electron microscopy showing high magnification of the central part of a 3 mm-wide twisted/dried ribbon that was diagonally cut with a scalpel. Scale bar; 20 μm.

microscopy has shown that our biological thread can be cut very clearly (figure 4(H)), and high magnification imaging of diagonal cross-sections revealed the presence of stratified lamellae connected by fibrillar structures within the thread (figure 4(I)).

3.4. Production of the CAM-based sutures

For the production of CAM-based sutures, 2 and 3 mm-wide twisted/dried ribbons obtained from ovine CAM sheets cultured for 16 weeks were crimped in eyeless surgical needles with adequate dimensions for vascular applications (curve: 180°, length: 13 or 17 mm, wire diameter: 0.53 mm, and hole diameter: 0.33 or 0.36 mm). Indeed, crimping an eyeless surgical needle with our twisted/dried CAM-based ribbons was successfully realized using a standard pneumatic crimping machine which is used for clinically available synthetic suture production (figures 5(A)–(D) and S2, video 1). The rigidity of the dried threads and their small diameters allowed easy insertion into the hole of the needle (figures 5(A) and (B), video 1). The CAM-based suture materials were flexible and easy to handle (figure 5(D)). In addition, these materials were compatible with standard knotting techniques (figure 5(E)). The strength of the needle attachment was measured using a pull test (figure 5(F)). Dried sutures made with 2 and 3 mm-wide CAM-based ribbons showed non-significant detachment force (figure 5(F); 2 mm-wide: 2.1 N *vs.* 3 mm-wide: 2.6 N). Unlike dried threads that slipped out of the needle during the pull tests, suture material ruptures were observed when the test was realized on ribbons that were rehydrated for 45 min, suggesting that the needle attachment strength is superior to the max force of the suture material.

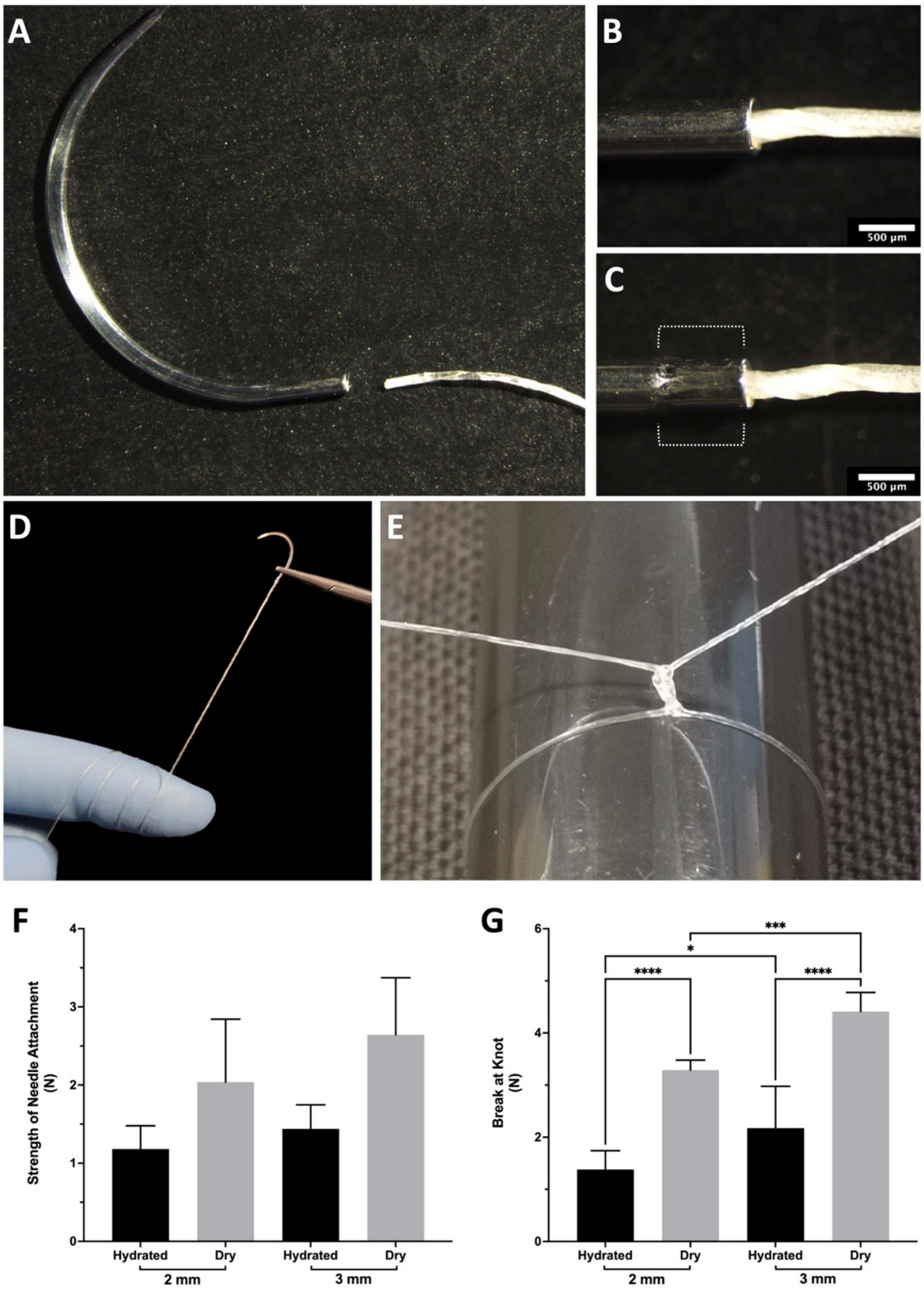

Figure 5. Production and characterization of biological sutures. (A)–(C) A twisted and dried CAM-based ribbon were inserted within the hole of a surgical needle and crimped using a pneumatic attaching machine to produce biological sutures. The white dotted parentheses show the crimping area of the needle. Scale bars; 500 μm for (B) and (C). (D) Macroscopic image showing the flexibility and the handling of a 2 mm-wide hydrated ribbon crimped in a surgical needle. (E) Macroscopic image of a knot repetition made with a 2 mm-wide hydrated ribbon. (F) The strength of the needle attachment was measured for the biological sutures made with 2 or 3 mm-wide CAM-based ribbons that were hydrated or twisted/dried. Data collected from hydrated sutures corresponded to suture material break. (G) Break at knot was also measured for hydrated and dry biological suture materials composed of 2 or 3 mm-wide CAM-based ribbons (significant differences: * $P < 0.05$; ** $P < 0.01$; *** $P < 0.001$ **** $P < 0.0001$).

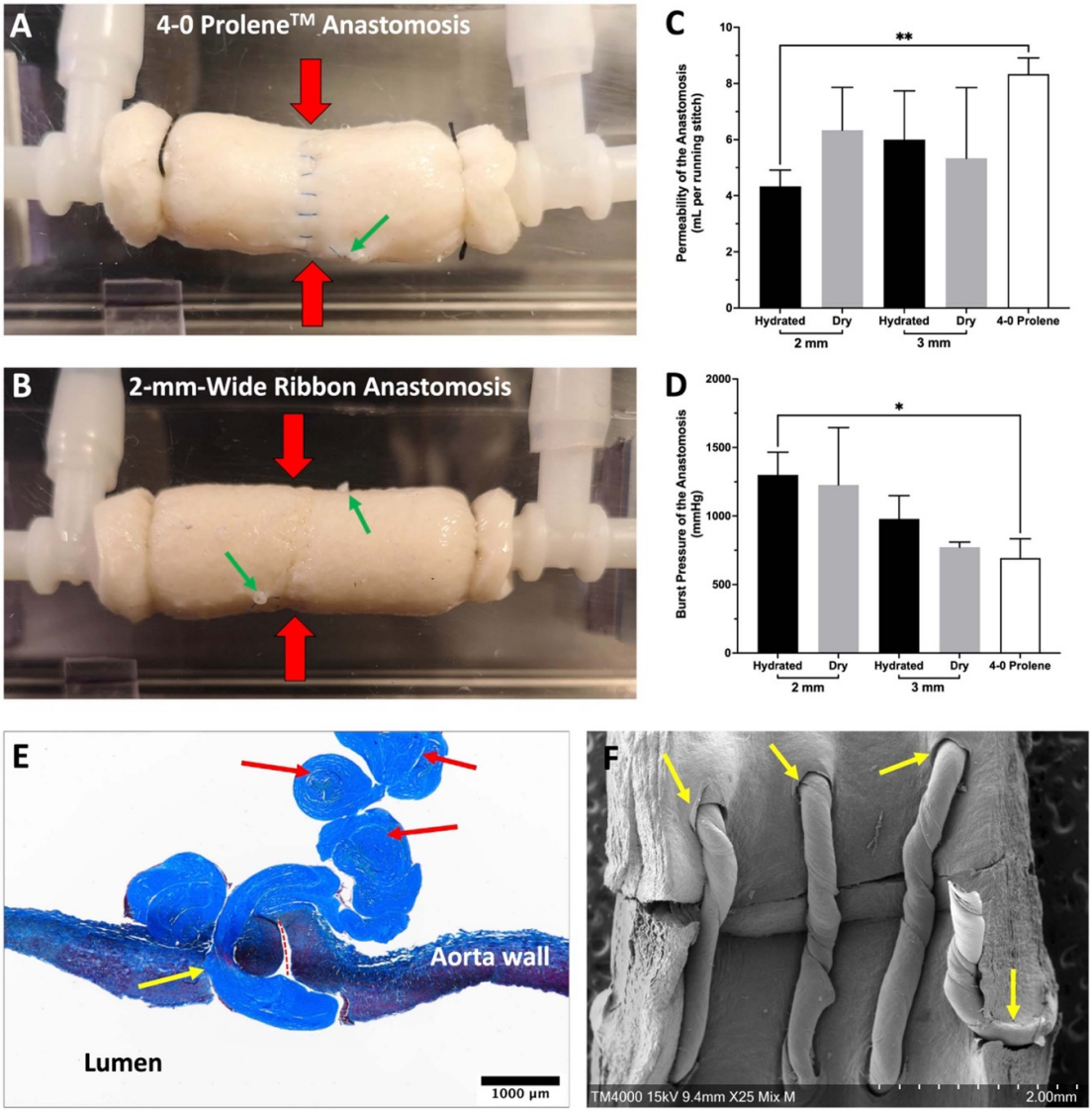

Figure 6. *Ex vivo* anastomosis evaluations. (A) and (B) Freshly explanted ovine thoracic aortas were anastomosed *ex vivo* using synthetic 4-0 Prolene™ or CAM-based suture materials (red arrows). Then, aortas were connected to custom-made testing systems to evaluate permeability and burst pressure. Collateral vessels (green arrows) were ligatured to prevent leakage. (C) Permeability assay was realized on aortas anastomosed with 2 and 3 mm-wide ovine CAM-based ribbons that were hydrated or twisted/dried and 4-0 Prolene™ sutures. Data demonstrated a significant difference in water leakage for aortas anastomosed with the 2 mm-wide ribbon sutures compared to 4-0 Prolene™ (significant difference: ** $P < 0.01$). (D) Then, burst pressure was measured on these anastomosed aortas. Results revealed that aortas anastomosed with the biological sutures showed higher burst pressures than the 4-0 Prolene™ suture (significant difference: * $P < 0.05$). (E) Cross-section of paraffin-embedded anastomosis stained with Masson's trichrome showing a close apposition of the aorta (red dotted line), the terminal knot composed of a repetition of simple knots (red arrows), and the passage of the biological suture (2 mm-wide ribbon) through the wall of the aorta (yellow arrow). Scale bar; 1000 μm. (F) Scanning electron microscopy showing the inner surface of the aorta at the anastomosis and the tight tissue apposition to suture material in the vascular wall (yellow arrows). Scale bar; 2 mm.

3.5. Breaking load

A breaking load assay was realized to evaluate the resistance of the suture material after making a simple knot (figure 5(G)). As expected, results showed that the knot resistance significantly increases with the width of the ribbon whether the suture material is hydrated (2 *vs.* 3 mm-wide hydrated ribbons: * $P < 0.05$) or dry (2 *vs.* 3 mm-wide twisted/dried ribbons: *** $P < 0.001$). Furthermore, data demonstrated that the twisting/drying of the CAM-based ribbons resulted in a significant augmentation of the thread resistance to knotting for the 2 (137%, **** $P < 0.0001$) and 3 mm-wide (103%, **** $P < 0.0001$) ribbon models.

3.6. *Ex vivo* evaluations of aorta anastomoses realized with CAM-based sutures

Anastomoses of animal thoracic aortas were realized with CAM-based sutures (2 and 3 mm wide ribbons) and compared to anastomoses made with a standard synthetic 4-0 Prolene™ suture (figure 6(A)). Biological sutures were either twisted and dried, which rehydrated only during the procedure, or fully rehydrates ribbons. Figure 6(B) shows the

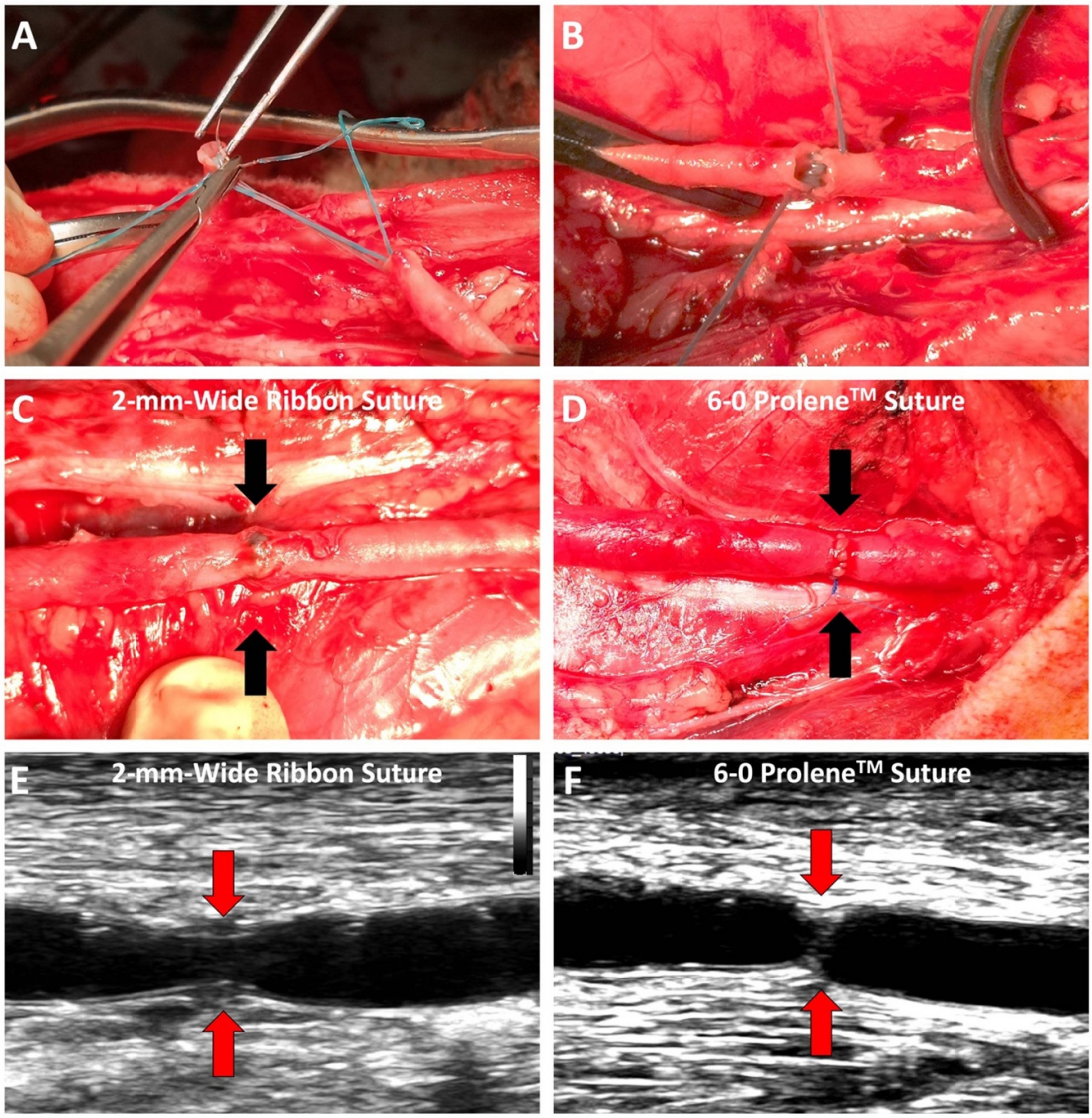

Figure 7. *In vivo* anastomosis evaluation. (A) and (B) A 2 mm-wide hydrated CAM-based ribbon suture (colored in blue) was compatible with standard surgical manipulations and a parachute approach for the termino-terminal anastomosis of the carotid in sheep models. (C) The anastomosis (black arrows) was successfully realized in a clinically relevant setting with complete hemostasis. (D) Termino-terminal anastomoses (black arrows) realized with standard 6-0 Prolene™ suture were used as references. (E) and (F) Ultrasound imaging confirmed the absence of thrombus, blood leakage, and major stenosis 10 min after closing the anastomoses (red arrows) for both suture models.

macroscopic appearance of an anastomosis performed with hydrated sutures (2 mm-wide ribbon) and using a parachute technique with standard surgical instruments. The procedure was straightforward, even though this was performed using the weakest suture configurations, and produced a uniform connection with good tissue approximation. Water permeability assay and burst pressure tests revealed that using CAM-based sutures resulted in a more leak proof and stronger anastomosis when compared to standard synthetic sutures (figures 6(C) and (D)). Masson's trichrome coloration (figure 6(E)) and scanning electron microscopy (figure 6(F)) demonstrated that our CAM-based sutures completely filled the hole created by the needle (shown by the yellow arrows in figures 6(E) and (F)), explaining the low level of water permeability. After bursting testing, we observed that all ruptures were at the level of the running stitches, and no breaks of the suture materials or the terminal knots were noted (figure S3).

3.7. *In vivo* termino-terminal carotid anastomosis

To demonstrate the usability of an allogeneic biological suture in clinically relevant application, we realized termino-terminal carotid anastomoses in sheep models. Because of the small diameter of the carotid (4 to 5 mm-diameter, similar to humans), we used a model of hydrated ribbon with an initial width of 2 mm crimped with a surgical needle with adequate dimensions (curve: 180°, length:

13 mm, wire diameter: 0.53 mm, and hole diameter: 0.33 mm). To better visualized the biological suture material during imaging, the CAM-based ribbons were colored in blue. As demonstrated *ex vivo*, our biological suture was compatible with a parachute approach, a technique commonly used in vascular surgery (figures 7(A) and (B), videos 2 and 3). The termino-terminal carotid anastomoses were perfectly secured with standard knots (six repetitions) (video 4). In addition, no leakage was observed after blood flow re-establishment (figure 7(C)), even after applying manual tension on the anastomosed vessel (video 5). These results were similar to those obtained when anastomoses were realized using standard 6-0 Prolene™ sutures (figure 7(D)). Ultrasound imaging of the anastomoses realized with biological sutures confirmed the absence of thrombus or hematoma formation and the presence of a smooth luminal surface (figure 7(E)), as observed in reference anastomosed realized with 6-0 Prolene™ suture (figure 7(F)). Taken together, these data confirmed the efficiency of our biological sutures in a clinically relevant setting.

4. Discussion

Most surgical procedures require suture materials for tissue repair or closing [1]. The worldwide surgical suture market was recently evaluated at $4 billion in 2021 [32]. With the aging population, the number of surgeries will considerably increase, and the need for suture materials is expected to reach $7 billion by 2030 with a compound annual growth rate of 6.2%. Ideal suture material must be mechanically relevant for the targeted application and accepted by the patient's body without generating an inflammatory reaction. Synthetic sutures made of polymers, such as Prolene™ or Vicryl™, remain the gold standard for surgery [4, 5]. However, these synthetic materials are recognized as foreign bodies and generate inflammatory reactions [6–8]. In this study, we developed an innovative suture made of a non-denatured biological material that has already shown superior biological properties in humans (tissue integration, remodeling, resist infection, and does not elicit an immune response) [26–28]. After characterizing the mechanical properties of hydrated CAM-based ribbons, we have shown that twisted/dried ribbons obtained from CAM sheet can be attached to an eyeless surgical needle to produce biological sutures using a standard manufacturing approach (video 1). In addition, we demonstrated that CAM-based sutures are compatible with standard surgical instruments and techniques for vessel anastomoses.

While we focused on developing sutures for vascular surgery applications, the versatility of the CAM allows manufacturing suture materials with adapted diameters and mechanical properties for other surgical applications, such as skin wound closure or valve repair. A previous study showed that CAM sheet characteristics, such as strength, thickness, and hydroxyproline quantity, correlate positively [24]. Here, we demonstrated that these CAM characteristics (perforation strength, hydroxyproline quantity, thickness, max force, and strain at break) are also related to the time of culture. These findings give a better understanding of CAM production for generating CAM material with adequate strength and size for targeted applications.

As predicted, CAM-based ribbons from human or ovine origins displayed lower mechanical properties than clinical Prolene™ sutures for the same diameter. Indeed, the 10th edition of the Ph. Eur. determined that two-gauge (or 3-0 USP size) Prolene™ threads must show a maximum force equal to or greater than 9 N, which is 4.7 times higher than our strongest ribbons (16 week-old human ribbons with an initial width of 3 mm: 1.9 N) [33]. It also recommends a minimum force of needle attachment of 6.8 N for the two-gauge Prolene™ sutures, which is 2.6 times higher than our strongest sutures (16 week-old ovine ribbons with an initial width of 3 mm that have been twisted and dry: 2.6 N) [33]. Among biological sutures, catgut is the closest to compare with our CAM-based sutures. Indeed, this suture is a resorbable biomaterial composed of thin longitudinal collagenous ribbons obtained from bovine, goats, or sheep intestinal mucosa twisted and joined together as a filament [34]. Compared to the catgut mechanical requirements defined in the 10th edition of the Ph. Eur. [33], our CAM-based ribbons showed lower mechanical properties (max force, needle/thread attachment, and knot resistance). This would be expected since catgut is generally chemically treated with chromium salts, a tanning agent, to enhance its mechanical properties and extend its integrity and absorption time [34]. Despite these mechanical differences, our CAM-based sutures resisted standard surgical handling. Indeed, we demonstrated that we can use this biomaterial to anastomose vessels in a clinically relevant setting (see videos 2–5). In the future, we can imagine twisting two or three CAM-based ribbons with a smaller width to generate stronger multifilament-like biological sutures with the same diameter. Since catgut suture material has been banned for human use in Europe and Japan due to concerns regarding bovine spongiform encephalopathy transmission (mad-cow disease) [35], there are no more biological sutures in these markets, and our CAM-based suture represents an innovative replacement.

Other research groups have developed biological threads, not necessarily to produce a suture but for other biological textile applications [25]. For example, Zhang *et al* developed a filament composed of type I collagen extracted from rat-tail tendons to produce small-diameter knitted vascular grafts [36]. Compared to our CAM-based material, which displayed max forces ranging between 0.6 N (2 mm-wide

ribbon from 8 week-old CAM sheet) to 1.9 N (3 mm-wide ribbon from 16 week-old CAM sheet), their denatured collagen thread showed a much lower breaking force of 0.3 N in wet condition, even considering that their thread is 1.6-times larger than our strongest biological suture (3 mm-wide ribbon made from a 16 week-old CAM sheet). In addition, Zeugolis *et al* developed a biological thread composed of denatured and extruded type I collagen with a breaking force of 0.2 N (in wet condition) with the approximately same diameter (≈300 μm) [37] as our biological thread made of a 3 mm-wide hydrated ribbon obtains from a 16 week-old CAM sheet. These strength differences can be explained by the complex structural composition of the CAM material, which is made of at least 70 ECM-related proteins including several of them playing important mechanical roles (collagens, fibrillin, fibulins, etc.) [21, 24]. To improve the strength of denatured collagen threads, researchers tried different cross-linking techniques (chemical, physical, and biological) [37, 38]. While these methods of collagen ramification increased the strength of their threads, they negatively impacted the biological advantage of the collagen by reducing the cellular migration potential [38]. In addition, compared to our CAM material composed of a native-like collagenous structure which favor cell adhesion, this type of processed collagen will trigger an inflammatory reaction and be rapidly resorbed once implanted.

We compared *ex vivo* the mechanical performances of our CAM-based suture materials with a synthetic 4-0 Prolene™ suture to anastomose large arteries. Interestingly, our biological materials showed lower water permeability. The high flexibility and compressibility of our CAM material, which contains about 80% water, compared to rigid plastic materials, such as Prolene™, may explain the reduction of the water permeability. Indeed, our material was able to perfectly fill the needle hole and limit the space created by the tension of the thread. The bursting assay also showed favorable results for our CAM-based suture materials compared to Prolene™. Ruptures were observed at the level of the running stitches for each suture material (figure S3), suggesting that the rigidity of synthetic threads caused a significant shear stress during the pressure augmentation that cut the tissue and caused the failure. In contrast, the high flexibility of our CAM material may limit this shear stress.

While we already demonstrated that our CAM material does not elicit a chronic inflammatory reaction and shows slow remodeling subcutaneously in nude rats [30] and humans [28], the material was not evaluated in the conditions of a specific vascular suture. In this study, we realized a very short-term *in vivo* evaluation in sheep models of our CAM-based sutures that confirmed the validity of this approach. In future studies, the *in vivo* remodeling of the CAM-based sutures will be analyzed since this is the potentially revolutionary aspect of this approach. Indeed, this studies will include juvenile animals to assess the growth potential and the long-term remodeling of the CAM material for pediatric applications.

5. Conclusion

This study presents the first biological sutures made of CAM and demonstrates their potential for vascular surgery applications. Indeed, our biological sutures were compatible with standard vascular surgery techniques *ex vivo* and *in vivo*. *Ex vivo*, anastomoses made with these biological sutures displayed lower permeability and higher burst resistance than those made with Prolene™ sutures. *In vivo*, we successfully used our biological sutures for carotid anastomoses in a clinically relevant setting. Finally, we demonstrated that completely biological CAM-based sutures have the appropriate mechanical strengths for cardiovascular applications.

Data availability statement

All data that support the findings of this study are included within the article (and any supplementary files).

Acknowledgments

This work was supported by the French '*Agence Nationale de la Recherche* (ANR)' (Grant Number: ANR-21-CE17-0001-01); and the French Federation of Cardiology (FFC). PB received a scholarship from the '*Association Chirurgicale pour le Développement et l'Amélioration des Techniques de Dépistage et de Traitement des Maladies Cardio-vasculaires* (ADETEC)'. FK received a fellowship from the '*Fondation pour la Recherche Médicale* (FRM)' (Grant Number: SPF202004011810). The authors thanks Julien P Vitry from BioTis Laboratory, Virginie Loyer and Stéphane Bloquet from the IHU Liryc, as well as Romane Lesieur from the CIC-IT of Bordeaux for their technical supports.

Credit author statement

Paul Borchiellini: Methodology, Formal Analysis, Investigation, Data Curation. Adeline Rames: Methodology, Formal Analysis, Investigation, Data Curation. François Roubertie: Resource, Writing—Review & Editing. Nicolas L'Heureux: Conceptualization, Resources, Writing—Review & Editing. Fabien Kawecki: Writing—Original Draft, Conceptualization, Methodology, Formal Analysis, Investigation, Validation, Data Curation, Resources, Visualization, Supervision, Project Administration, Funding Acquisition.

Conflict of interest

Authors declare that they have no competing financial interests.

ORCID iDs

Nicolas L'Heureux https://orcid.org/0000-0001-8602-3948
Fabien Kawecki https://orcid.org/0000-0002-1409-623X

References

[1] Dennis C, Sethu S, Nayak S, Mohan L, Morsi Y and Manivasagam G 2016 Suture materials—current and emerging trends *J. Biomed. Mater. Res.* A **104** 1544–59
[2] Hochberg J, Meyer K M and Marion M D 2009 Suture choice and other methods of skin closure *Surg. Clin. North Am.* **89** 627–41
[3] Debus E S, Geiger D, Sailer M, Ederer J and Thiede A 1997 Physical, biological and handling characteristics of surgical suture material: a comparison of four different multifilament absorbable sutures *Eur. Surg. Res.* **29** 52–61
[4] Schmitz-Rixen T, Storck M, Erasmi H, Schmiegelow P and Horsch S 1991 Vascular anastomoses with absorbable suture material: an experimental study *Ann. Vasc. Surg.* **5** 257–64
[5] Calhoun T R and Kitten C M 1986 Polypropylene suture—is it safe? *J. Vasc. Surg.* **4** 98–100
[6] Aarnio P, Harjula A, Lehtola A, Sariola H and Mattila S 1988 Polydioxanone and polypropylene suture material in free internal mammary artery graft anastomoses *J. Thoracic Cardiovascular Surg.* **96** 741–5
[7] Vincent H F, Hatem J M, Upshur J and Sade R M 1983 Atrial wound healing with polyglycolic acid and polypropylene sutures *J. Thoracic Cardiovascular Surg.* **86** 150–3
[8] Lock A M, Gao R, Naot D, Coleman B, Cornish J and Musson D S 2017 Induction of immune gene expression and inflammatory mediator release by commonly used surgical suture materials: an experimental *in vitro* study *Patient Saf. Surg.* **11** 1–8
[9] Eickhoff R M *et al* 2019 Improved biocompatibility of profiled sutures through lower macrophages adhesion *J. Biomed. Mater. Res.* B **107** 1772–8
[10] Helmedag M, Heise D, Eickhoff R, Kossel K M, Gries T, Jockenhoevel S, Neumann U P, Klink C D and Lambertz A 2021 Cross-section modified and highly elastic sutures reduce tissue incision and show comparable biocompatibility: *in-vitro* and *in-vivo* evaluation of novel thermoplastic urethane surgical threads *J. Biomed. Mater. Res.* B **109** 693–702
[11] Dart A J and Dart C M 2017 Suture material: conventional and stimuli responsive *Comprehensive Biomaterials II* (Elsevier) pp 746–71
[12] Reimer J, Syedain Z, Haynie B, Lahti M, Berry J and Tranquillo R 2017 Implantation of a tissue-engineered tubular heart valve in growing lambs *Ann. Biomed. Eng.* **45** 439–51
[13] Ryu K J, Ahn K H and Hong S C 2014 Spontaneous complete migration of suture material after subcuticular continuous suture in cesarean section: a case report *BMC Surg.* **14** 4–6
[14] Foster J A, John K B, Castro E and Meisler D M 2000 Blepharoptosis surgery complicated by late suture migration *Am. J. Ophthalmol.* **130** 116–7
[15] Lee J, Oh S and Jeon M J 2021 Suture complication rates and surgical outcomes according to the nonabsorbable suture materials used in vaginal uterosacral ligament suspension: polyester versus polypropylene *J. Minim. Invasive Gynecol.* **28** 1503–7
[16] Mahesh L, Kumar V R, Jain A, Shukla S, Aragoneses J M, González J M M, Fernández-Domínguez M and Calvo-Guirado J L 2019 Bacterial adherence around sutures of different material at grafted site: a microbiological analysis *Materials* **12** 1–8
[17] Masini B D, Stinner D J, Waterman S M and Wenke J C 2011 Bacterial adherence to suture materials *J. Surg. Educ.* **68** 101–4
[18] Dineen P 1977 The effect of suture material in the development of vascular infection *Vasc. Endovascular Surg.* **11** 29–33
[19] Peck M, Gebhart D, Dusserre N, McAllister T N and L'Heureux N 2011 The evolution of vascular tissue engineering and current state of the art *Cells Tissues Organs* **195** 144–58
[20] Peck M, Dusserre N, McAllister T N and L'Heureux N 2011 Tissue engineering by self-assembly *Mater. Today* **14** 218–24
[21] Magnan L, Labrunie G, Marais S, Rey S, Dusserre N, Bonneu M, Lacomme S, Gontier E and L'Heureux N 2018 Characterization of a cell-assembled extracellular matrix and the effect of the devitalization process *Acta Biomater.* **82** 56–67
[22] Magnan L *et al* 2020 Human textiles: a cell-synthesized yarn as a truly "bio" material for tissue engineering applications *Acta Biomater.* **105** 111–20
[23] Torres Y, Gluais M, Da Silva N, Rey S, Grémare A, Magnan L, Kawecki F and L'Heureux N 2021 Cell-assembled extracellular matrix (CAM) sheet production: translation from using human to large animal cells *J. Tissue Eng.* **12** 204173142097832
[24] Kawecki F, Gluais M, Claverol S, Dusserre N, McAllister T N and L'Heureux N 2022 Inter-donor variability of extracellular matrix production in long-term cultures of human fibroblasts *Biomater. Sci.* **10** 3935–50
[25] Kawecki F and L'Heureux N 2023 Current biofabrication methods for vascular tissue engineering and an introduction to biological textiles *Biofabrication* **15** 022004
[26] L'Heureux N, McAllister T N and de la Fuente L M 2007 Tissue-engineered blood vessel for adult arterial revascularization *New Engl. J. Med.* **357** 1451–3
[27] Wystrychowski W, McAllister T N, Zagalski K, Dusserre N, Cierpka L and L'Heureux N 2014 First human use of an allogeneic tissue-engineered vascular graft for hemodialysis access *J. Vasc. Surg.* **60** 1353–7
[28] Wystrychowski W *et al* 2022 Long-term results of autologous scaffold-free tissue-engineered vascular graft for hemodialysis access *J. Vascular Access* 112972982210959
[29] Potart D, Gluais M, Gaubert A, Da Silva N, Hourques M, Sarrazin M, Izotte J, Mora Charrot L and L'Heureux N 2023 The cell-assembled extracellular matrix: a focus on the storage stability and terminal sterilization of this human "bio" material *Acta Biomater.* **166** 133–46
[30] Magnan L, Kawecki F, Labrunie G, Gluais M, Izotte J, Marais S, Foulc M P, Lafourcade M and L'Heureux N 2021 *In vivo* remodeling of human cell-assembled extracellular matrix yarns *Biomaterials* **273** 120815
[31] L'Heureux N *et al* 2006 Human tissue-engineered blood vessels for adult arterial revascularization *Nat. Med.* **12** 361–5
[32] Strategic Market Research 2022 Surgical sutures market by type (sutures, automated suturing devices, nonabsorbable sutures), material (hospitals, ambulatory surgical centers (ASCs), clinics & physician offices), application (cardiovascular surgeries, gynecological surgeries, general surgeries, ophthalmic surgeries, orthopedic surgeries, other surgeries), by geography, segment revenue estimation, forecast, 2021-2030 *Report ID* 81621365 (available at: www.strategicmarketresearch.com/market-report/surgical-sutures-market)
[33] Council of Europe 2019 *European Pharmacopeia* vol 1, 10th edn (European Directorate for the Quality of Medicines & HealthCare (EDQM))

[34] Walton M 1989 Strength retention of chromic gut and monofilament synthetic absorbable suture materials in joint tissues *Clin. Orthop. Relat. Res.* **242** 303–10
[35] Langley-Hobbs S J 2014 Sutures and general surgical implants *Feline Soft Tissue and General Surgery* (Elsevier) pp 105–16
[36] Zhang F, Xie Y, Celik H, Akkus O, Bernacki S H and King M W 2019 Engineering small-caliber vascular grafts from collagen filaments and nanofibers with comparable mechanical properties to native vessels *Biofabrication* **11** 35020
[37] Zeugolis D I, Paul G R and Attenburrow G 2009 Cross-linking of extruded collagen fibers-A biomimetic three-dimensional scaffold for tissue engineering applications *J. Biomed. Mater. Res.* A **89** 895–908
[38] Cornwell K G, Lei P, Andreadis S T and Pins G D 2007 Crosslinking of discrete self-assembled collagen threads: effects on mechanical strength and cell-matrix interactions *J. Biomed. Mater. Res.* A **80** 362–71